Original Paper

Cellular Physiology and Biochemistry

Cell Physiol Biochem 2011;28:1265-1278

Accepted: December 09, 2011

Activation of Volume Regulated Chloride Channels Protects Myocardium from Ischemia/reperfusion Damage in Second-Window Ischemic Preconditioning

Nathan D. Bozeat[1,*], Sunny Yang Xiang[1,*], Linda L. Ye[1], Tammy Y. Yao[1], Marie L. Duan[1], Dean J. Burkin[1], Fred S. Lamb[2] and Dayue Darrel Duan[1]

[1]the Department of Pharmacology, and Center of Biomedical Research Excellence, University of Nevada School of Medicine, Reno, Nevada, [2]the Department of Pediatrics, The University of Iowa, Iowa City
*These authors contributed equally to the current study

Key Words
Ischemia • Myocardial infarction • Hemodynamics • Ion channels • Genes

Abstract
Activation of volume regulated chloride channels (*VRCCs*) has been shown to be cardioprotective in ischemic preconditioning (IPC) of isolated hearts but the underlying molecular mechanisms remain unclear. Recent independent studies support that ClC-3, a ClC voltage-gated chloride channel, may function as a key component of the *VRCCs*. Thus, ClC-3 knockout (*Clcn3*$^{-/-}$) mice and their age-matched heterozygous (*Clcn3*$^{+/-}$) and wild-type (*Clcn3*$^{+/+}$) littermates were used to test whether activation of *VRCCs* contributes to cardioprotection in early and/or second-window IPC. Targeted disruption of ClC-3 gene caused a decrease in the body weight but no changes in heart/body weight ratio. Telemetry ECG and echocardiography revealed no differences in ECG and cardiac function under resting conditions among all groups. Under treadmill stress (10 m/min for 10 min), the *Clcn3*$^{-/-}$ mice had significant slower heart rate (648±12 bpm) than *Clcn3*$^{+/+}$ littermates (737±19 bpm, n=6, P<0.05). *Ex vivo* IPC in the isolated working-heart preparations protected cardiac function during reperfusion and significantly decreased apoptosis and infarct size in all groups. *In vivo* early IPC significantly reduced infarct size in all groups including *Clcn3*$^{-/-}$ mice (22.7±3.7% vs control 40.1±4.3%, n=22, P=0.004). Second-window IPC significantly reduced apoptosis and infarction in *Clcn3*$^{+/+}$ (22.9±3.2% vs 45.7±5.4%, n=22, P<0.001) and *Clcn3*$^{+/-}$ mice (27.5±4.1% vs 42.2±5.7%, n=15, P<0.05) but not in *Clcn3*$^{-/-}$ littermates (39.8±4.9% vs 41.5±8.2%, n=13, P>0.05). Impaired cell volume regulation of the *Clcn3*$^{-/-}$ myocytes may contribute to the failure of cardioprotection by second-window IPC. These results strongly support that activation of *VRCCs* may play an important cardioprotective role in second-window IPC.

Introduction

Ischemic preconditioning (IPC) is a phenomenon in which brief episodes of ischemia dramatically reduce myocardial infarction caused by a subsequent sustained ischemia [1]. IPC has an early phase (lasting 1-2 hours)

KARGER
Fax +41 61 306 12 34
E-Mail karger@karger.ch
www.karger.com

1015-8987/11/0286-1265$38.00/0

Accessible online at:
www.karger.com/cpb

Dayue Darrel Duan
Laboratory of Cardiovascular Phenomics , Department of Pharmacology
Center for Molecular Medicine CMM 303F
1664 N Virginia Street MS 318, Reno, Nevada 89557-0318 (USA)
Tel.+1775 784-4738, Fax +1775 784-1620, E-Mail dduan@medicine.nevada.edu

and a late phase or "second-window" (lasting 24-72 hours) of protection [2]. The signaling pathways involved in both early IPC (eIPC) and second-window IPC (swIPC) have been the subjects of intensive studies in the last 25 years [3-6].

Ischemia causes myocardial damage and leads to infarction through necrosis and programmed cell death (apoptosis) [6, 7]. Recent studies in cardiac and noncardiac cells have demonstrated that both the necrotic cell volume increase (NVI) and the apoptotic cell volume decrease (AVD) are closely regulated by the volume-regulated chloride (Cl^-) channels (VRCCs) or the cell swelling-activated Cl^- current ($I_{Cl,swell}$), [8-10] suggesting that VRCCs may be intimately linked to IPC through regulation of cell volume homeostasis and thus necrotic and apoptotic events. The first evidence that $I_{Cl,swell}$ was involved in IPC came from a study by Diaz et al., which demonstrated that Cl^- channel blockers 5-nitro-2-(3-phenylpropyl-amino) benzoic acid (NPPB) and indanyloxyacetic acid 94 (IAA-94) not only blocked the hypo-osmotic cell swelling induced current but also prevented the protection of isolated rabbit heart by IPC and hypo-osmotic stress [11]. Later studies from the same group provided further evidence to support the notion that $I_{Cl,swell}$ may be an important end-effector in IPC [12, 13] and it was believed that enhanced cell volume regulation may be a key mechanism for IPC protection [14]. These observations by Diaz et al., however, were seriously questioned by Heusch et al. [15, 16]. In an attempt to further confirm the effects of the same Cl^- channel blockers on both Cl^- channel activity in isolated ventricular myocytes and cardioprotection by IPC in isolated perfused rabbit heart, Heusch et al. found that the channel-blocking concentrations of both NPPB and IAA-94 were toxic in isolated perfused rabbit hearts, as evidenced by cessation of cardiac contraction and massive infarction, neither agent could be tested against IPC's anti-infarct effect [16]. The doses used in the report of Diaz et al. [11] did not affect coronary flow, heart rate and developed pressure, and also failed to prevent the infarct size reduction of IPC [16]. Similar results were obtained with an additional VRCCs blocker, 4, 4'-diisothiocyanostilbene-2,2'-disulfonic acid (DIDS) [16]. At this point, therefore, at least two important questions remain unanswered: 1) whether VRCCs play a causal role in IPC protection; 2) whether VRCCs are involved in eIPC or swIPC [2] if activation of $I_{Cl,swell}$ is important in IPC protection.

The effort to confirm the causal role of VRCCs in IPC has been hampered by the fact that the currently available Cl^- channel blockers lack specificity to any particular subgroup of Cl^- channels that are concomitantly expressed in the same cardiac cell [11, 13, 15, 16]. Recently, a great deal of experimental evidence from many laboratories strongly supports that ClC-3, a member of the ClC voltage-gated Cl^- channel superfamily, may be responsible for a key component of the native $I_{Cl,swell}$ in cardiac myocytes and many other tissues [8, 17-30]. Many of these published studies also link ClC-3 to cell volume regulation and apoptosis, [8, 17, 21-28] further reinforcing a potential role of ClC-3 in IPC. Using gene targeting technique to specifically inactivate ClC-3 gene expression in the mouse provides a unique and powerful approach to directly address the question whether VRCCs play a role in both eIPC and swIPC. In this study, therefore, we applied both in vitro IPC of isolated working heart [31] and *in vivo* mouse eIPC and swIPC model [2] to a ClC-3 knockout ($ClCn3^{-/-}$) murine line [26, 32] and their wild-type ($ClCn3^{+/+}$) and heterozygous ($ClCn3^{+/-}$) littermates. Our results indicate that targeted inactivation of ClC-3 gene prevented cardioprotective effects of swIPC but not of eIPC, suggesting that VRCCs may contribute differently to eIPC and swIPC, while VRCCs may be of neglect in eIPC, they may be important cardioprotective mediator in swIPC.

Materials and Methods

All experimental procedures were performed according to the *Guide for the Care and Use of Laboratory Animals* (US National Institute of Health publication No.85-23, revised 1996) and were in compliance with the institutional guidelines for animal care and use, approved by the University of Nevada Institutional Animal Care and Use Committee.

ClC-3 knockout ($Clcn3^{-/-}$) mice

Homozygous $Clcn3^{-/-}$ mice were generated at the Transgenic Center at the University of Nevada, Reno by mating heterozygous ($Clcn3^{+/-}$) breeders [26, 32] to $Clcn3^{+/-}$ siblings. These mouse mutants have been backcrossed on a C57/BL6 genetic background before heterozygous crossing to obtain the knockout ($Clcn3^{-/-}$) and their heterozygous ($Clcn3^{+/-}$) and wild-type ($Clcn3^{+/+}$) littermates [26, 32]. Male $Clcn3^{-/-}$ offspring of 8~16 weeks old and their age-matched male $Clcn3^{+/-}$ and $Clcn3^{+/+}$ littermates were used in this study. Genotypes of the mice were confirmed by polymerase chain reaction (PCR) on tail DNA using a three-primer assay resulting in a 750 base-pair (bp) band for $Clcn3^{-/-}$, a 280 bp band for $Clcn3^{+/+}$, and both bands for $Clcn3^{+/-}$. All animals had unrestricted access to standard chow and drinking water and were housed at constant room temperature (24±1°C) with a 12-hour (hr) light/12-hr dark cycle.

Isolated Langendorff and working heart preparations

Cardiac hemodynamic parameters were recorded from isolated Langendorff and working heart preparations continuously during the experiment and analyzed off-line by HSE data acquisition system (HSE HAEMODYN, Harvard Apparatus) as described previously [31, 33]. Briefly, hearts were removed rapidly from mice anesthetized with pentobarbital sodium (50 mg/kg, intraperitoneal injection). The aorta was cannulated with a cannula connected to the HSE isolated heart perfusion system (Model IH-1, Harvard Apparatus, Inc. Halliston, MA). Retrograde (Langendorff) perfusion was started instantly with modified Krebs-Henseleit buffer, which contained (in mmol/L): NaCl 118.0, KCl 4.7, $CaCl_2$ 2.5, $MgSO_4$ 1.2, KH_2PO_4 1.2, $NaHCO_3$ 25.0, pyruvate 2.0, glucose 11.0, EDTA-Na_2 0.5. Buffer was continuously bubbled with 95% O_2 and 5% CO_2 (pH 7.4, 37 °C) throughout the perfusion period. The left atrium was then cannulated and the hearts were perfused antegradely through the atrial cannula (working-heart mode, afterload 60 mmHg, preload 10 mmHg). Left ventricular pressure (LVP), left ventricular developed pressure (LVDP), and left ventricular end-diastolic pressure (LVEDP) were measured by a Millar tip catheter (1.4/0.8F pressure transducer, Millar) inserted into the left ventricular cavity through aorta or an open-ended PE-50 polyethylene cannula (O.D.=0.965 mm) inserted into the left ventricular cavity through the apex. Measurements of functional performance (aortic pressure, LVP, LVEDP, LVDP, first derivative of left ventricular developed pressure ±dP/dt and heart rate) were recorded continuously during the experiment and analyzed off-line by HSE data acquisition system. Cardiac output (CO) was calculated as the sum of coronary flow (CF) and aortic outflow collected during perfusion.

Assessment of tissue injury and viability

Total global ischemia by clamping both atrial inflow and aortic outflow was used for induction of sustained ischemia as well as for IPC. Myocardial tissue injury was determined by measuring infarct size using TTC staining as described previously [31, 33]. At the end of the experimental protocols, the hearts were perfused in the Langendorff mode for an additional 80 min and then frozen at -80 °C, transversely cut into ~600 μm slices and stained with 1% triphenyl tetrazolium chloride (TTC) in phosphate buffer (pH 7.4) at 37 °C for 15 min. After fixation in 10% neutral buffered formaldehyde overnight, the slices were scanned and saved as JPEG files. The viable myocardium stained deep red and necrotic tissues remained pale. The entire risk area (the sum of total ventricular area minus cavities) was calculated in pixels using computer software (SimplePCI, Compix, Inc, Cranberry Township, PA) and infarct areas were compared to the entire area at risk in a gray scale fashion [31, 33].

Caspase-3 measurement

The activated caspase-3 in the heart was measured using anti-active caspase 3 polyclonal antibody (ab13847, Abcam) and sodium dodecyl sulfate/polyacrylamide gel electrophoresis (SDS-PAGE) and immuno-blotting as described previously. At the end of protocol, ventricles of the heart were frozen in liquid nitrogen and the total protein from the ventricles was isolated, and resolved in 1X RIPA buffer (1% Triton X-100, 50 mM NaCl, 10 mM NaF, 1 mM Na_3VO_4, 5 mM EDTA, 10 mM Tris pH 7.6, 2 mM PMSF). Protein solution was mixed at 3:1 with 4 X Laemmli sample buffer (Bio-Rad) and incubated at 95°C for 5 min. The proteins were then fractionated by SDS-PAGE and electrotransferred to a nitrocellulose membrane. After washing, the membrane was blocked with odyssey blocking buffer (LI-COR) for 1 hr at RT. The membrane was then incubated overnight in the primary rabbit anti-active Caspase 3 polyclonal antibody (ab13847,abcam) at 4°C in the blocking buffer. After washing, the blots were incubated with secondary goat anti-rabbit 680 antibody (Li-Cor) (1:100,000) and imaged using the with Odyssey infrared imaging system and analyzed with Odyssey software (V1.2, LI-COR). GAPDH (glyceraldehyde-3-phosphate dehydrogenase) was used as the internal control.

Terminal deoxynucleotidyl transferase-mediated dUTP nick end labeling (TUNEL) assay

In order to identify apoptotic cells containing DNA fragments, the tissue samples (serial 8 μm cryosections) were labeled by immunohistochemical staining using terminal deoxynucleotidyl transferase (TdT) and fluorescein conjugated nucleotides with the in situ cell death detection kit (Roche Applied Science) as described in the manufacturer's instructions. Negative control sections were prepared without the TdT enzyme and continuing with the staining. Labelled nuclei were identified from the negative nuclei counterstained by propidium iodide (PI) (Vector Laboratories, Inc. Burlingame, CA) and counted after being photographed under a fluorescence microscope at 40x magnification. The percentage of TUNEL positive nuclei (expressed as % of positive nuclei/all nuclei) was determined by counting the PI labelled nuclei and TUNEL positive nuclei present in the endocardium.

Cell volume measurement

LV myocytes were isolated from adult (8-weeks) *Clcn3*$^{+/+}$ and *Clcn3*$^{-/-}$ hearts using methods as described previously [34, 35]. After the enzyme treatment, the myocytes were dissociated and stored for 30 min in a modified KB solution [35, 36] containing (mmol/L): 70 potassium glutamate, 20 KCl, 1 $MgCl_2$, 10 KH_2PO_4, 10 taurine, 10 EGTA, 10 glucose, 10 β-hydroxybutric acid, 10 Hepes, and 1mg/mL bovine albumin; pH 7.2 with KOH; 300 mOsm/kg with mannitol. Then 4 ml of the myocytes were transferred to a tube and 2 nL/mL of Di-8-ANEPPS (Molecular Probes, Invitrogen) were added. The myocytes were incubated in dark at room temperature (22-24 °C) for 30 min. Within the same day of isolation and treatment with Di-8-ANEPPS the myocytes were examined under fluorescent microscope for the measurement of cell volume changes under isotonic and hypotonic conditions. All cells studied were rod shaped, exhibited clear cross-striations, and lacked any visible blebs under isotonic conditions. Viable ventricular myocytes were stained red by Di-8. Hypotonic (230 mOsm/kg H_2O, measured by freezing-point depression) bath solutions contained (mmol/L) NaCl 100, $MgCl_2$ 1, $CaCl_2$ 1, $BaCl_2$ 2, NaH_2PO_4 0.33, CsCl 10, HEPES 10, glucose 5.5, pH 7.4. The isotonic and hypertonic bath solutions were the same as the hypotonic solution except the osmolarity was adjusted to 300 mOsm/kg H_2O and 360

mOsm/kg H_2O by adding mannitol. Cells were photographed under microscope (10x) every min while they were perfused with isotonic solution for 5 min and then with hypotonic solutions for 20 min. Cell dimensions (length and width) were measured with SimplePCI (Compix Inc., Cranberry Township, PA, USA). The cell volume (V) was estimated with assumed right cylindrical geometry according to the following equation: $V=\pi L(W/2)^2$, where V, L, and W are cell volume, length, and width, respectively [34, 37]. Experiments were conducted at room temperature (22°C to 24°C).

Radiotelemetry electrocardiography (ECG) recording system

During the various protocols of this study, ECG, heart rate (HR), activity, and body temperature were measured, collected and stored to hard disk of an IBM-compatible computer using the Data Sciences International radiotelemetry data acquisition system (Dataquest A.R.T. version 2.2, Data Sciences International, St Paul, MN). The mice were anesthetized with sodium pentobarbital (50~100 mg/kg, ip) and an incision (1.5 cm) was made along the midline immediately caudal to the xyphoid space for the subcutaneous placement of the body of the implantable transmitter (ETA-F20). The two insulated stainless-steel biopotential leads (0.5 mm diameter) of the transmitter were cut to the appropriate length and placed subcutaneously into the small incisions (0.5 cm) in the lead II configuration (negative lead to the right shoulder and the positive lead to the left of the xyphoid space and caudal to the rib cage). The device was included in the closing suture (4-0 non-absorbable) to prevent displacement. The mice were allowed to recover on a heating pad for 24hr. Measurements were taken every two hours for 20 seconds for up to five weeks. ECG data analyses were performed off-line using Physiostat ECG analysis software, version 3.1 (Data Sciences International). The QT interval was corrected for heart rate (QTc) using the following formula: $QTc = QT/(RR/100)^{1/2}$ as previously described [38].

Treadmill Exercise Regimen

The animals in all groups were trained twice a week on rodent Treadmill Simplex II (Columbus Instruments, Columbus, Ohio) for 2 weeks before the implantation of the telemetry probe. The exercise regimen started 2 days (48 hrs) after surgery. The mice were allowed to acclimate to the treadmill (0-2 m/min) for 10 min prior to each trial. The mice were run at a speed of 5 m/min for 10 min followed by 10 m/min for 10 min finishing with 15 m/min for 10 minutes. ECG was monitored with the telemetry system every two hours for 10 minutes at rest and continually during the treadmill exercise test.

Echocardiography

Transthoracic M-mode echocardiogram was used to assess left ventricle (LV) performance before and after IPC protocols using a GE Vingmed System Five Ultrasound, EchoPAC software version 6.2 with a 12 MHz transducer (GE Vingmed Ultrasound A/S, Horten, Norway). The mice were anesthetized with sodium pentobarbital (~25 mg/kg, ip). The dose of the anesthetics was chosen to maintain a heart rate at >600 beat-per-minute (bpm). After a good-quality two-dimensional image was obtained M-mode images of the left ventricle were recorded. All measurements were performed using the leading edge–to–leading edge convention adopted by the American Society of Echocardiography [39]. End-diastolic (ed) volume and end-systolic (es) volume were calculated for the following: inter ventricular septum (IVS), left ventricular diameter (LVD), and left ventricular posterior wall (LVPW). The left ventricular ejection fraction ($LVEF = [(LVDed)^3 - (LVDes)^3]/LVDed^3$) and left ventricular fractional shortening (%FS = [(LVDed - LVDes)/LVDed] x 100%) were calculated with the analysis program incorporated on the ultrasound machine.

In vivo IPC experimental protocols

Clcn3$^{+/+}$, *Clcn3*$^{+/-}$, and *Clcn3*$^{-/-}$ mice were randomly divided into eight early IPC (eIPC) and second-window IPC (swIPC) groups with various experimental protocols as described in details in the Results section. The mice were anesthetized with sodium pentobarbital (50 mg/kg, ip). Additional doses of pentobarbital were administered during the protocol as required to maintain anesthesia (up to a maximum total dose of 100 mg/kg, ip). The animals were intubated and ventilated with room air (approximately 21% oxygen with a tidal volume of 200 µl at a rate of 200 breaths/min), using a MiniVent rodent ventilator (Model 845, Hugo Sachs Elektronik, March Hugstettn, Germany). Body temperature was controlled through a heating pad, to maintain at ~37°C. Surface 12-lead ECG was recorded throughout the experiments on a Gould ACQ-7700 recorder (Gould Instrument Systems, Valley View, OH). A left thoracotomy was performed, the heart exposed, and the pericardium was removed from the left ventricle. The left anterior descending (LAD) coronary artery 2~3 mm from the tip of the left atrium was occluded with a prolene 8.0-silk suture. Successful coronary occlusion was verified by the development of a pale color in the distal myocardium through the use of a Surgical Microscope system (Applied Fiberoptics, Southbride, Massachusetts) and by S-T segment elevation and QRS widening on the ECG. Blood flow was restored by releasing the ligature. Successful reperfusion was confirmed when the bright red color of the left ventricle and the ECG returned to normal. The chest was closed and the mice were removed from the ventilator and allowed to recover on the heating pad, or sacrificed prior to removal from the ventilator depending on the IPC protocols (see below).

The experimental protocols for *in vivo* eIPC and swIPC models are described as follows (see also description in the corresponding figures):

1) eIPC (see Fig. 3): Age-matched *Clcn3*$^{+/+}$, *Clcn3*$^{+/-}$, and *Clcn3*$^{-/-}$ mice were subjected to a) 30-min ischemia followed by 40 min reperfusion (I/R 40 min, Group 1); b) 30-min ischemia followed by 24 hr reperfusion (I/R 24 hr, Group 2); c) open chest with no I/R for 24 min followed by 30 min ischemia and 40 min open chest reperfusion and then closed chest 24 hr reperfusion (sham control, Group 3); or d) 3 cycles of 4 min ischemia and 4 min reperfusion (IPC) followed by 30 min ischemia and 40 min open chest reperfusion and then closed chest 24 hr reperfusion (IPC, Group 4).

2) swIPC (see Fig. 4): Age-matched *Clcn3*$^{+/+}$, *Clcn3*$^{+/-}$,

	Clcn3$^{+/+}$ (n = 6)		*Clcn3*$^{+/-}$ (n = 6)		*Clcn3*$^{-/-}$ (n = 6)	
	Rest	Exercise	Rest	Exercise	Rest	Exercise
HR (bpm)	602±15	738±17$^{\#\#\#}$	607±16	729±20$^{\#\#\#}$	608±8	648±4$^{***,\#\#}$
PQ (ms)	7.3±1.6	39.4±0.6	36.2±1.5	38.6±0.8	34.0±0.5	34.3±0.7***
RR (ms)	99.9±2.4	81.5±1.9$^{\#\#\#}$	98.1±2.2	82.2±1.8$^{\#\#\#}$	98.6±1.4	92.5±0.3$^{***,\#\#}$
QRS (ms)	12.7±0.3	14.5±0.3	13.8±0.6	14.2±0.7	14.0±0.5	14.1±0.5
ST (ms)	15.2±0.4	12.5±0.2$^{\#\#\#}$	14.8±0.5	12.3±0.3$^{\#\#\#}$	14.1±0.5	14.1±0.2***
QT (ms)	55.3±1.4	52.7±0.5	55.9±1.1	52.4±0.4$^{\#}$	56.7±0.6	59.3±0.5$^{***,\#\#}$
QTc (ms)	55.4±1.9	58.4±1.2	56.2±1.5	57.6±1.1	57.1±1.8	61.7±0.6$^{*,\#}$

Table 1. Telemetry recordings of Lead II ECG from *Clcn3*$^{+/+}$, *Clcn3*$^{+/-}$, and *Clcn3*$^{-/-}$ mice $^{\#}$. Heart rate (HR), PQ, QRS, QT, ST and RR segments on a standard lead II ECG were measured from age-matched mice under rest and treadmill exercise (10 m/min for 10 min) conditions. QTc = QT/(RR/100)$^{1/2}$. $^{*}P < 0.05$, $^{**}P < 0.01$, $^{***}P < 0.001$ *Clcn3*$^{-/-}$ vs *Clcn3*$^{+/+}$ *or ClCn3*$^{-/+}$. $^{\#}P < 0.05$, $^{\#\#}P < 0.01$, $^{\#\#\#}P < 0.001$ Exercise vs Rest

and *Clcn3*$^{-/-}$ mice were subjected to a) open chest with no I/R for 24 min on Day 1, followed by 30 min ischemia and 40 min open chest reperfusion on Day 2 (sham control, Group 1); b) 3 cycles of 4 min ischemia and 4 min reperfusion (IPC) on Day 1 followed by 30 min ischemia and 40 min open chest reperfusion on Day 2, c) open chest with no I/R for 24 min on Day 1, followed by 30 min ischemia and 40 min open chest reperfusion on Day 2 and then closed chest 24 hr reperfusion (sham control, Group 3); or d) 3 cycles of 4 min ischemia and 4 min reperfusion (IPC) on Day 1 followed by 30 min ischemia and 40 min open chest reperfusion on Day 2 and then closed chest 24 hr reperfusion (IPC, Group 4).

Measurement of the myocardial infarction size

At the end of each protocol, 1.0 ml of 1% 2,3,5-triphenyltetrazolium chloride (TTC) solution (0.15M triss buffer, pH 7.8, at 4ºC) was injected as a bolus via the aorta into the left ventricular chamber. The coronary artery was reoccluded, and 0.2 ml of a 5% phthalol dye solution was then injected as a bolus via the aorta into the left ventricular chamber. The heart was then removed and the LV isolated. The weight of whole heart and the LV were measured. The isolated LV was placed into the -80º freezer for one hour. The LV was cut transversely into five slices from base to apex, and stored in 37% formaldehyde for 24hrs. Color digital images of both sides of each slice were obtained with a Sony DSC-F707 digital camera (Sony, Minokamo, Japan). The area under risk (tissue unstained by phthalol dye) and the infarct size (white tissue unstained by TTC) of the LV were outlined on each color image and quantified by a blinded observer using the image processing and analysis (IPA) module of Simple PCI image analysis software (Compic, Inc., USA) [31]. The percent infarction was calculated for each slice, and reported as the percent of infarct (white) tissue divided by the total area under risk (white and red).

Statistical Analysis

All group data is presented as mean±SEM. Statistical comparisons were performed either by Student's *t* test when only two groups were compared or by multiple analysis of variance (MANOVA) with Scheffé contrasts for group data. A 2-tailed probability value of P=0.05 was considered statistically significant.

	Clcn3$^{+/+}$ (n=13)	*Clcn3*$^{+/-}$(n=14)	*Clcn3*$^{-/-}$ (n=13)
HR (bpm)	602±8	598±12	586±7
IVSd (mm)	0.67±0.04	0.66±0.02	0.67±0.01
LVIDd (mm)	2.50±0.16	2.46±0.09	2.39±0.08
LVPWd (mm)	0.74±0.04	0.70±0.03	0.71±0.02
IVSs (mm)	0.85±0.07	0.84±0.06	0.88±0.06
LVIDs (mm)	0.76±0.06	0.78±0.05	0.80±0.05
LVPWs (mm)	0.92±0.06	0.82±0.06	0.85±0.05
LVEF	0.92±0.01	0.93±0.01	0.91±0.01
%FS	67.9±1.8	68.8±1.2	66.6±1.7

Table 2. M-mode echocardiogram before surgery on age-matched *Clcn3*$^{+/+}$, *Clcn3*$^{+/-}$, and *Clcn3*$^{-/-}$ mice.

Results

Cardiovascular Phenotypes of Clcn3$^{-/-}$ *mice under rest and stressed conditions*

Before the application of ischemia/reperfusion (I/R) and IPC protocol to *Clcn3*$^{-/-}$ mice we first addressed the question whether the disruption of *ClC-3* gene alone would cause significant changes in basic cardiovascular functions of *Clcn3*$^{-/-}$ mice and their *Clcn3*$^{+/-}$ and *Clcn3*$^{+/+}$ littermates under rest conditions. At the age of 8 weeks, the body weight of the *Clcn3*$^{-/-}$ mice (20.50±0.31g, n=32) was significantly less than *Clcn3*$^{+/-}$ (28.24±0.35g, n=31, P<0.05) and *Clcn3*$^{+/+}$ (27.72±0.48g, n=39, P<0.05) mice. The heart weight/body weight (mg/g) ratio (5.10±0.08, n=32), and the LV weight/body weight (mg/g) ratio (0.80±0.02) of the *Clcn3*$^{-/-}$ mice were not, however, significantly different from those of their *Clcn3*$^{+/-}$ (5.13±0.12 and 0.79±0.03, n=31, P>0.05) and *Clcn3*$^{+/+}$ (5.14±0.07 and 0.81±0.01, n=39, P>0.05) littermates, respectively.

	Clcn3$^{+/+}$		*Clcn3*$^{+/-}$		*Clcn3*$^{-/-}$	
	Control (n=6)	eIPC (n=7)	Control (n=5)	eIPC (n=6)	Control (n=6)	eIPC (n=6)
LVEF (pre)	0.95±0.04	0.95±0.02	0.97±0.01	0.96±0.01	0.96±0.01	0.96±0.01
LVEF (post)	0.70±0.05**	0.89±0.01$^{\#}$	0.72±0.05**	0.87±0.02$^{\#}$	0.70±0.04**	0.88±0.01$^{\#}$

Table 3. Comparison of left ventricular ejection fraction (LVEF) before (pre) and after (post) prolonged ischemia in age-matched *Clcn3*$^{+/+}$, *Clcn3*$^{+/-}$, and *Clcn3*$^{-/-}$ mice. §M-mode echocardiograph was taken when mice in either Control (Group 3) or eIPC (Group 4) were anaesthetized (pentobarbital 25 mg/kg). Experimental protocols are described in Fig. 1A. ** $P < 0.01$, LVEF (post) vs LVEF (pre) in Control groups. $^{\#}$ $P < 0.05$, LVEF (post) in eIPC groups vs LVEF (post) in Control groups.

To investigate whether ClC-3 knockout resulted in abnormal cardiac function transthoracic M-mode echocardiogram was used to examine the LV wall thickness and function of age-matched *Clcn3*$^{+/+}$, *Clcn3*$^{+/-}$, and *Clcn3*$^{-/-}$ mice before the application of experimental surgery protocols. To eliminate the influence of reduction in the heart rate on cardiac performance under anesthetized status a small dose of sodium pentobarbital (~25 mg/kg, ip) was used to maintain the heart rate at ~600 bpm during recordings. Evaluation of systolic and diastolic LV wall thickness (IVS and LVPW), chamber dimension (LVID), and contractile function (LVEF and %FS) revealed no statistically significant differences between age-matched *Clcn3*$^{+/+}$, *Clcn3*$^{+/-}$, and *Clcn3*$^{-/-}$ mice (see Table 1).

A radiotelemetry system was used to continuously monitor the ECG, body temperature and activity of age-matched *Clcn3*$^{+/+}$, *Clcn3*$^{+/-}$, and *Clcn3*$^{-/-}$ mice were under conscious conditions. No significant differences in HR, PQ, QRS, QT, or ST intervals on a standard lead II ECG were found at rest in these littermates (see Table 2), although the *Clcn3*$^{-/-}$ mice were more active than *Clcn3*$^{+/+}$ and *Clcn3*$^{+/-}$ mice. To detect possible phenotypic changes in cardiac electrophysiology of *Clcn3*$^{-/-}$ mice that are not readily apparent at rest we exercised the mice on treadmill with telemetry implants for up to five weeks. Under treadmill exercise stress (10 m/min for 10 min), HR of *Clcn3*$^{+/+}$ and *Clcn3*$^{+/-}$ mice was significantly increased, accompanied with a significant decrease in QRS and QT intervals. However, exercise increased HR to a much smaller extent and caused no significant changes in QRS, QT, and QTc in the *Clcn3*$^{-/-}$ mice (Table 2).

Effect of targeted inactivation of ClC-3 gene on IPC in isolated working heart

Previous studies in the isolated rabbit heart showed controversial results on the role of VRCCs in IPC when using Cl^- channel blockers [11, 16]. So, it is important to test whether IPC protect the heart from ischemia and reperfusion damage in the isolated *Clcn3*$^{-/-}$ heart. Age-matched male *Clcn3*$^{+/+}$ and *Clcn3*$^{-/-}$ mice were randomly divided into two groups with the experimental protocols as described in Figure 1A to examine the effect of IPC on ischemia-induced myocardial infarct size. As shown in Figure 1B, IPC caused a significant recovery of the heart function in all three groups of age-matched mice, suggesting targeted inactivation of the ClC-3 gene failed to prevent IPC in isolated mouse heart.

Effect of targeted inactivation of ClC-3 gene on apoptosis

It has been demonstrated previously that apoptosis and necrosis are the major cell death pathways involved in I/R injury and myocardial infarction and that both IPC can reduce the I/R-induced apoptosis [6, 7]. To test whether activation of ClC-3 Cl^- channels is important in the IPC-mediated inhibition of apoptosis, isolated Langendorff and working heart preparations of *ex vivo* IPC models were applied to age-matched male *Clcn3*$^{+/+}$ and *Clcn3*$^{-/-}$ mice. Hearts from the *Clcn3*$^{+/+}$ and *Clcn3*$^{-/-}$ mice were separated into 3 groups: perfusion control group, I/R group with 30 min ischemia followed by 5 hrs reperfusion, and IPC group with 3 cycles of 5 min I/R followed by 30 min ischemia then followed by 5 hr reperfusion. In the control group 5 hrs of perfusion resulted in little caspase 3 activation. But after 30 min ischemia 5 hrs of reperfusion caused a significant increase in caspase-3 activation in the *Clcn3*$^{+/+}$ and *Clcn3*$^{-/-}$ hearts. The I/R induced caspase-3 activation, however, was significantly reduced by IPC in both *Clcn3*$^{+/+}$ and *Clcn3*$^{-/-}$ hearts to a level similar to that of *Clcn3*$^{+/+}$ hearts in the control group (Fig. 1C), indicating that the IPC-induced inhibition of apoptosis in these hearts was not affected by knockout of ClC-3.

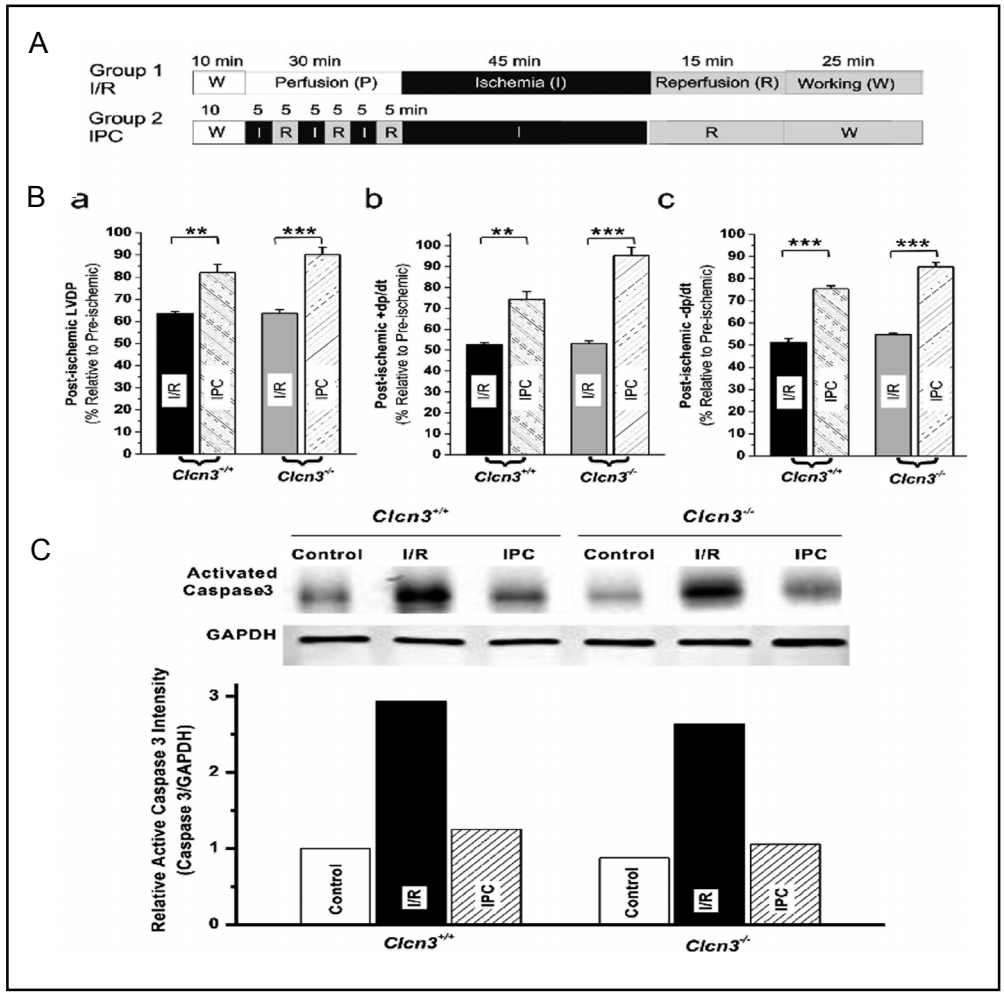

Fig. 1. Effects of ClC-3 gene knockout on ischemic preconditioning in isolated working mouse heart. A. Experimental protocol. B. Recovery of left ventricular contractile (a and b) and relaxation (c, -dp/dt) function of *Clcn3*$^{+/+}$ and *Clcn3*$^{-/-}$ mice after 45 min ischemia and 40 min reperfusion. C. Western blots (WB) analysis of activated caspase-3 in an isolated perfusion heart model for either *Clcn3*$^{+/+}$ or *Clcn3*$^{-/-}$ mice exposed to reperfusion alone (control), ischemia/reperfusion (I/R) or ischemic preconditioning (IPC) protocols. After control (5 hr perfusion), I/R (30 min ischemia /5 hr reperfusion) or IPC (3 cycles of 5 min I/R right before the 30 min ischemia/5 hr reperfusion) treatments, hearts lysates from each group were obtained and subjected to WB analysis for activated caspase-3. GAPDH was immunoblotted as a loading control. Relative active caspase-3 density after normalized to GAPDH is shown on the bottom.

To further confirm the observations on the effects of *ClC-3* knockout on the apoptosis of cardiac myocytes TUNEL assays were performed to detect apoptotic cells under I/R and IPC conditions. Figure 2A shows a representative image of TUNEL assays in mouse heart sections. In these studies, the reperfusion time was increased to >360 min to allow DNA damage to develop. In the control hearts not subject to global I/R, 420 min of perfusion caused the development of some TUNEL-positive (TN-P) nuclei in the epicardium, but none was detected in deeper layers of the myocardium (data not show). I/R caused 17.8±4.9% (n=6) and 28.4±2.2% (n=6) TN-P nuclei in the *Clcn3*$^{+/+}$ and *Clcn3*$^{-/-}$ hearts (P=0.077), respectively. IPC significantly reduced TN-P nuclei in the *Clcn3*$^{+/+}$ (1.4±0.2, n=6, P<0.01), and also the *Clcn3*$^{-/-}$ hearts (2.1± 0.5%, n=6, P<0.001) (Fig. 2B). These results further support ClC-3 may not be very important for the IPC-mediated inhibition of apoptosis in the heart.

To further determine whether ClC-3 encoded *VRCCs* play any functional role in IPC, we applied the *in vivo* eIPC and swIPC models, which are considered gold-standard for IPC, to the *Clcn3*$^{+/+}$, *Clcn3*$^{+/-}$, and *Clcn3*$^{-/-}$ mice.

The effect of targeted inactivation of ClC-3 gene on eIPC

Age-matched male *Clcn3*$^{+/+}$, *Clcn3*$^{+/-}$, and *Clcn3*$^{-/-}$ mice were randomly divided into four eIPC groups with the experimental protocols as described in Figure 3A. A surface standard lead II ECG was recorded throughout the surgery process to assess successful occlusion and reperfusion of the LAD coronary artery. M-mode echocardiogram was used to estimate the changes in cardiac function after surgery on *Clcn3*$^{+/+}$, *Clcn3*$^{+/-}$, and *Clcn3*$^{-/-}$ mice. As shown in Figure 3B, prolonged ischemia and reperfusion caused a significant decrease in cardiac function as estimated by LVEF while eIPC significantly protected the cardiac function from prolonged ischemia/reperfusion damage with a significantly blunted decrease in LVEF compared to the control groups in all *Clcn3*$^{+/+}$, *Clcn3*$^{+/-}$, and *Clcn3*$^{-/-}$ mice.

Consistent with the changes in cardiac function, eIPC significantly reduced the infarct size of LV myocardium caused by sustained ischemia for 30 min and reperfusion for 40 min or 24 hrs in all *Clcn3*$^{+/+}$, *Clcn3*$^{+/-}$, and *Clcn3*$^{-/-}$ mice (Fig. 3C). These results indicate that targeted inactivation of ClC-3 gene failed to affect the cardioprotective effect of eIPC on mouse heart, suggesting that ClC-3 encoded VRCCs may play little role in the eIPC cadioprotection.

The effect of targeted inactivation of ClC-3 gene on late IPC

Age-matched *Clcn3*$^{+/+}$, *Clcn3*$^{+/-}$, and *Clcn3*$^{-/-}$ mice were randomly divided into four swIPC groups with the experimental protocols as described in Figure 4A. Mice in Group 1 (I/R 40-min sham control) underwent 24-min open chest sham followed by 24-hr closed chest recovery and on the second day the mice underwent a 30-min prolonged ischemia followed by 40-min open chest reperfusion. Mice in Group 2 (I/R 40-min swIPC) underwent a three-cycle IPC (a sequence of 4-min ischemia and 4-min reperfusion) followed by 24-hr closed chest recovery, and then a 30-min prolonged ischemia followed by a 40-min open chest reperfusion. Mice in Group 3 (I/R 24-hr sham control) underwent a 24-min open chest sham followed by 24-hr closed chest recovery and on the second day the mice underwent a 30-min prolonged ischemia followed by 40 min open chest reperfusion and a 24-hr closed chest reperfusion. Mice in Group 4 (I/R 24-hr swIPC) underwent a 24-min IPC followed by 24-hr closed chest recovery and on the second day the mice underwent a 30 min prolonged ischemia followed by 40-min open chest reperfusion and 24-hr closed chest reperfusion. As shown in Figure 4B, prolonged ischemia and reperfusion cause a significant decrease in LVEF and %FS in all *Clcn3*$^{+/+}$, *Clcn3*$^{+/-}$, and *Clcn3*$^{-/-}$ mice in the control groups (Groups 1 and 3). There was no significant difference between Group 1 (I/R 40-min) and Group 3 (I/R 24-hr). In the swIPC groups (Groups 2 and 4) of *Clcn3*$^{+/+}$ and *Clcn3*$^{+/-}$ mice, the reduction of LVEF and FS was significantly less than in the control groups, suggesting a protection of the cardiac function of these mice by swIPC against ischemia and reperfusion. In the swIPC group of *Clcn3*$^{-/-}$ mice, however, no significant difference was observed in the reduction in LVEF and %FS compared to the control group after swIPC (Fig. 4B). Similarly, swIPC significantly reduced myocardial infarction in *Clcn3*$^{+/+}$ and *Clcn3*$^{+/-}$ mice but failed to reduce myocardial infarct size in *Clcn3*$^{-/-}$ mice (Fig. 4C). These results indicate that targeted inactivation of ClC-3 gene abolished the cardioprotective effect of swIPC on mouse heart and suggest that ClC-3 encoded VRCCs may play an important role in swIPC.

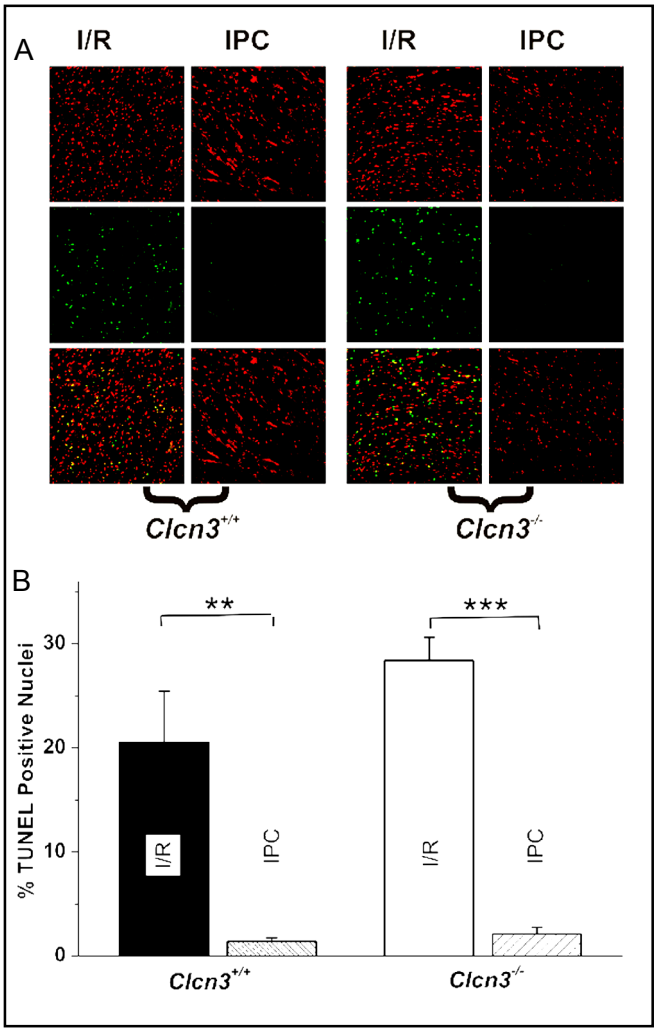

Fig. 2. TUNEL assay of the effects of ClC-3 gene knockout on ischemia/reperfusion and ischemic preconditioning in isolated working mouse heart. A. Representative images of heart longitudinal sections of TUNEL staining for each group of treatments: I/R (30 min ischemia/5 hr reperfusion) or IPC (3 cycles of 5 min I/R right before the 30 min ischemia/5 hr reperfusion). Green: TUNEL stained nuclei; red, propidium iodide (PI) stained nuclei. B. Relative percentage of TUNEL positive (TP) cells calculated as 100% (count of TP/count of PI), data presented as mean ± SEM, n=6, ** P<0.01, *** P=0.001.

The effect of targeted inactivation of ClC-3 gene on cell volume regulation

Ischemia and reperfusion cause myocardium infarction through necrosis and apoptosis [6, 7, 40]. Irreversible isosmotic cell swelling or necrotic volume increase (NVI) due to ATP depletion under conditions of ischemia

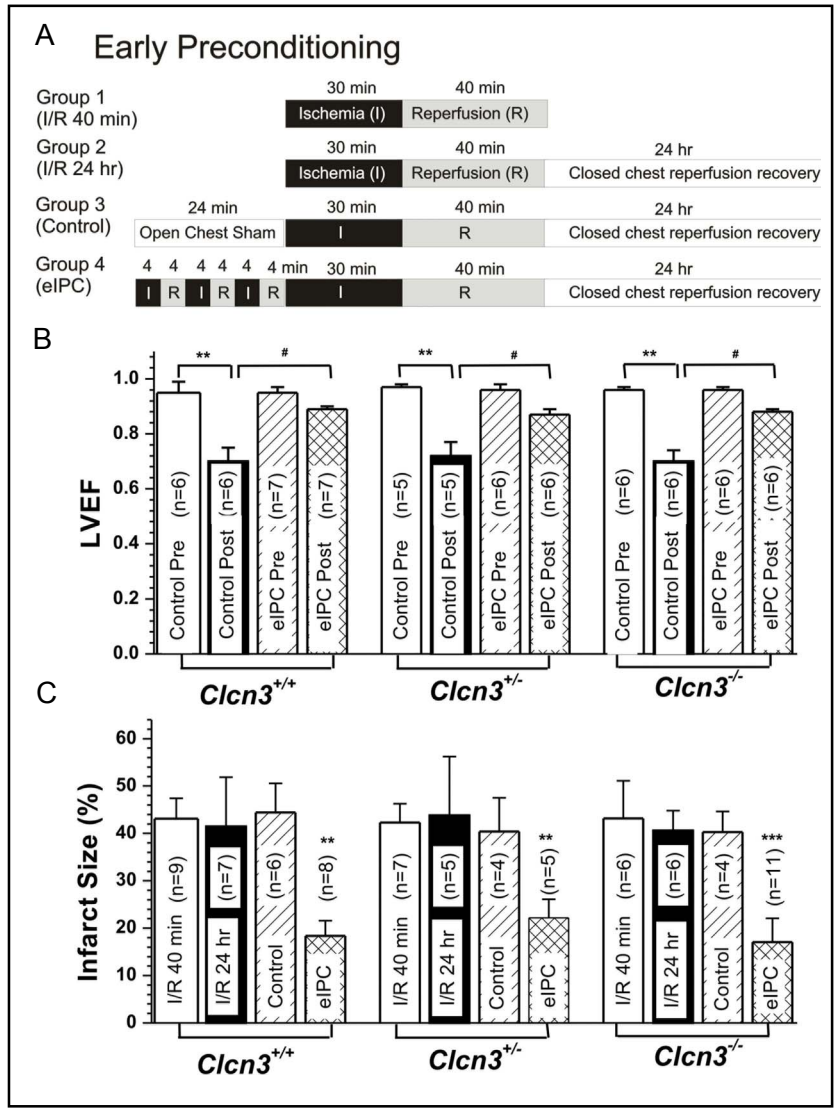

Fig. 3. Effect of ClC-3 gene knockout on early ischemic preconditioning in mouse heart. A. Experimental protocols. Age-matched *Clcn3*$^{+/+}$, *Clcn3*$^{+/-}$, and *Clcn3*$^{-/-}$ mice after ischemia and reperfusion of 40 min (I/R 40 min, Group 1) or 24 hr (I/R 24 hr, Group 2), open chest sham (Control, Group 3), or IPC (Group 4). B. Early IPC on left ventricular ejection fraction (LVEF, mean±SEM) of *Clcn3*$^{+/+}$, *Clcn3*$^{+/-}$, and *Clcn3*$^{-/-}$ mice. M-mode echocardiograph was taken from anaesthetized (pentobarbital 25 mg/kg) mice in either Control (Group 3) or eIPC (Group 4) before (pre) or after (post) prolonged ischemia/reperfusion as shown in panel A. ** $P < 0.01$, LVEF (post) vs LVEF (pre) in Control groups. $^{\#}$ $P < 0.05$, LVEF (post) in eIPC groups vs LVEF (post) in Control groups. C. Early IPC on infarct size (mean±SEM) of left ventricles of *Clcn3*$^{+/+}$, *Clcn3*$^{+/-}$, and *Clcn3*$^{-/-}$ mice. eIPC significantly reduced the infarct size in all groups of mice (** $P<0.01$, *** $P<0.001$). ClC-3 knockout caused no significant changes in IPC protection ($P > 0.05$ vs *Clcn3*$^{+/+}$ and *Clcn3*$^{+/-}$, MANOVA).

or hypoxia may cause cell rupture, i.e., necrotic cell death. On the other hand, isosmotic cell shrinkage or apoptotic volume decrease (AVD) is an integral part of apoptosis. Both NVI and AVD have been found to be closely regulated by VRCCs [8-10] and ClC-3 [8, 17, 21-28]. Therefore, it is important to examine whether knockout of ClC-3 gene causes any changes in cell volume regulation. As shown in Figure 5, exposure of the ventricular myocytes isolated from *Clcn3*$^{+/+}$ mouse heart to hypotonic superfusion solution caused a quick increase in cell volume (solid circles), which reached a plateau within 10 min and then began to decrease (RVD) back to the normal cell volume as in the isotonic solutions after approximately 15 min in the continued presence of hypotonic solution. Exposure of these cells to a hypertonic superfusion solution caused further decrease in cell volume (shrinkage). In ventricular myocytes from *Clcn3*$^{-/-}$ mice, cell volume also increased soon after exposure to hypotonic superfusion solutions but the maximum increase in cell volume (158.3±11.8%, n=4) was significantly larger than that of *Clcn3*$^{+/+}$ mice (121.6±9.6%, n=5, P<0.05) at a faster rate (solid squares). Although an initiation of RVD also began to occur after 10 min in the hypotonic superfusion solution the RVD never reached to the normal cell volume and a second increase in cell volume quickly occurred and all cells ruptured due to an excessive increase in cell volume in the hypotonic solutions. These data suggest that one functional consequence of ClC-3 knockout in the heart is an impaired RVD in individual myocytes.

Discussion

In this study we applied well-established *in vivo* eIPC and swIPC models to a *Clcn3*$^{-/-}$ murine line to directly

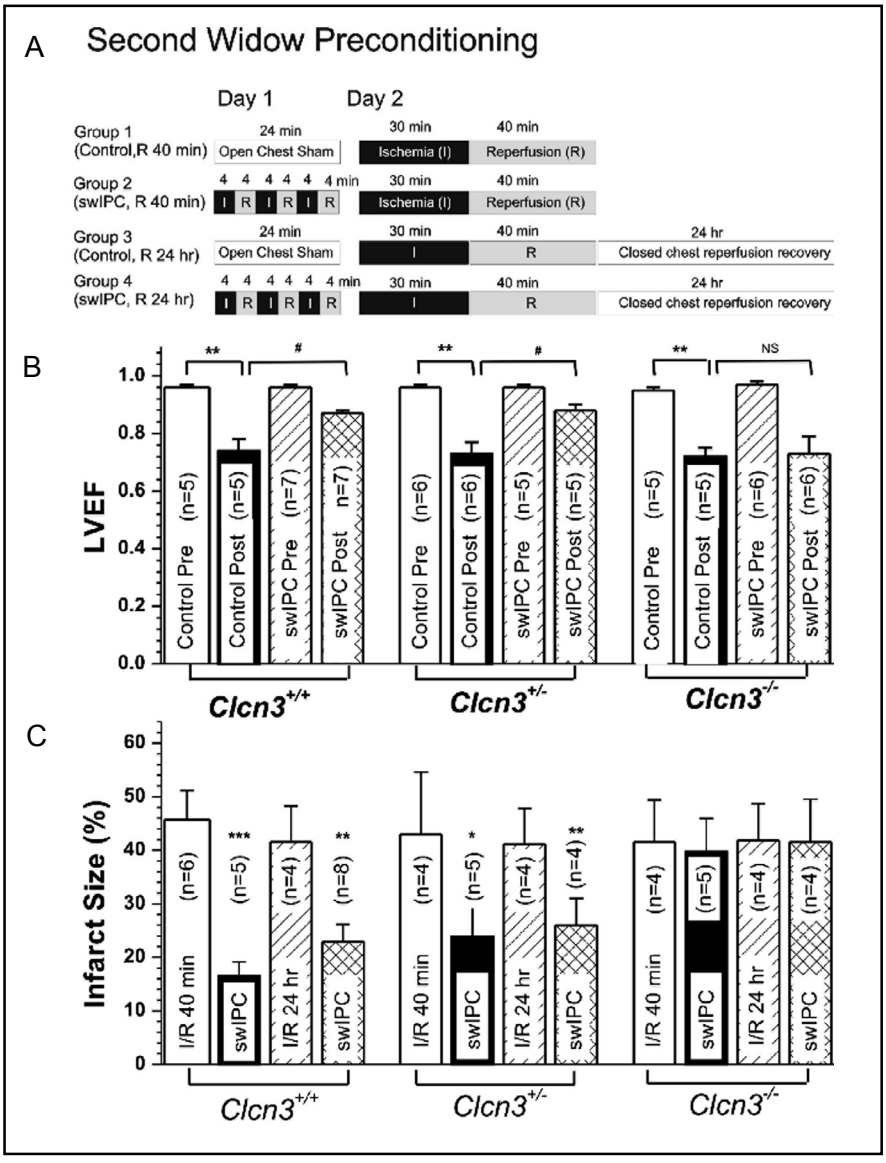

Fig. 4. Effect of ClC-3 gene knockout on second window ischemic preconditioning (swIPC) in mouse heart. A. Experimental protocols. Age-matched *Clcn3*$^{+/+}$, *Clcn3*$^{+/-}$, and *Clcn3*$^{-/-}$ mice after ischemia and reperfusion of 40 min (I/R 40 min, Group 1) or IPC (Group 2), and 24 hr (I/R 24 hr, Group 3) or IPC (Group 4).). B. swIPC on left ventricular ejection fraction (LVEF, mean±SEM) of *Clcn3*$^{+/+}$, *Clcn3*$^{+/-}$, and *Clcn3*$^{-/-}$ mice. M-mode echocardiograph was taken from anaesthetized (pentobarbital 25 mg/kg) mice in either Control (Group 3) or swIPC (Group 4) before (pre) or after (post) prolonged ischemia/reperfusion as shown in panel A. ** $P < 0.01$, LVEF (post) vs LVEF (pre) in Control groups. $^{\#}$ $P < 0.05$, ^{NS} $P > 0.05$, LVEF (post) in swIPC groups vs LVEF (post) in Control groups. C. swIPC significantly reduced the infarct size in *Clcn3*$^{+/+}$ and *Clcn3*$^{+/-}$ mice but not in *Clcn3*$^{-/-}$ mice, suggesting that ClC-3 gene knockout prevented the protection of the heart from ischemia/reperfusion damage. (* $P<0.05$, ** $P<0.01$; *** $P<0.001$). ClC-3 knockout caused no significant changes in IPC protection ($P > 0.05$ vs *Clcn3*$^{+/+}$ and *Clcn3*$^{+/-}$, MANOVA).

	Clcn3$^{+/+}$		*Clcn3*$^{+/-}$		*Clcn3*$^{-/-}$	
	Control (n=5)	swIPC (n=7)	Control (n=6)	swIPC (n=5)	Control (n=5)	swIPC (n=6)
LVEF (pre)	0.96±0.01	0.96±0.01	0.96±0.01	0.96±0.01	0.95±0.01	0.97±0.01
LVEF (post)	0.74±0.04**	0.87±0.01$^{\#}$	0.73±0.04**	0.88±0.02$^{\#}$	0.72±0.03**	0.73±0.06

Table 4. Comparison of left ventricular ejection fraction (LVEF) before (pre) and after (post) prolonged ischemia in age-matched *Clcn3*$^{+/+}$, *Clcn3*$^{+/-}$, and *Clcn3*$^{-/-}$ mice. §§ M-mode echocardiography was taken when mice in Control (Group 3) or swIPC (Group 4) were anaesthetized (pentobarbital 25mg /kg to maintain HR at >600 bpm). Experimental protocols are described in Figure 4A. ** $P < 0.01$, LVEF (post) vs LVEF (pre) in Control groups. $^{\#}$ $P < 0.05$, LVEF (post) in swIPC groups vs LVEF (post) in Control groups.

address the question whether the ClC-3 encoded VRCCs are involved in both eIPC and swIPC. Our results strongly suggest that VRCCs may be an important mediator in swIPC protection although they may play a little role in eIPC.

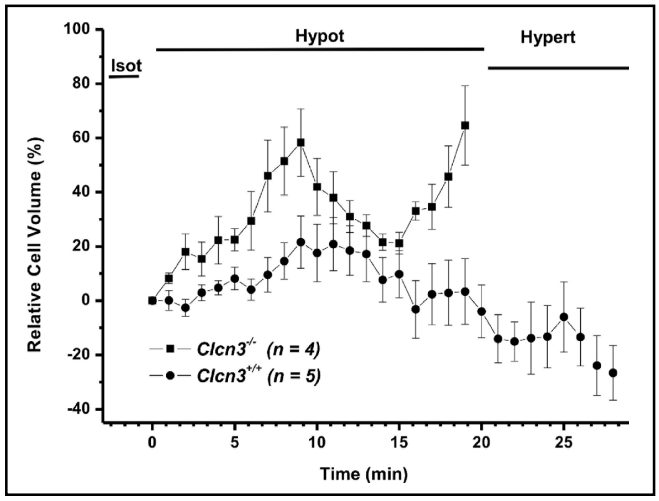

Fig. 5. Hypotonic-induced cell swelling and regulatory volume decrease in ventricular myocytes from *Clcn3*$^{+/+}$ and *Clcn3*$^{-/-}$ mice. At Time 0, the isotonic (300 mOsmol) bath solution was changed to a hypotonic (220 mOsmol) solution and, thereafter, cells were superfused continuously with the hypotonic solution for 20 min before switched to hypertonic (360 mOsmol) solution. Relative cell volumes (%) were normalized against cell volume measured in isotonic solution right before hypotonic superfusion.

Phenotype of Clcn3$^{-/-}$ *mice*

Targeted disruption of ClC-3 gene causes extensive hippocampal neurodegeneration and retina malformation resulting in blindness and lead to a proportional decrease in body weight through an unknown mechanism [32, 40, 41]. Therefore, before the application of the IPC models to the *Clcn3*$^{-/-}$ mice, we carefully examined the cardiovascular phenotype of these mice using echocardiography and telemetry ECG measurements. To eliminate the possible effect of anesthesia-induced changes in heart rate on cardiac performance the echocardiography recordings were made at similar heart rate. In addition, telemetry was used to assess the cardiovascular phenotype of the mice in non-anesthetized and unrestricted conditions. Under resting conditions no significant differences were observed in heart rate, PQ, QRS, QT, ST intervals or body temperature in age-matched *Clcn3*$^{-/-}$, *Clcn3*$^{+/-}$, and *Clcn3*$^{+/+}$ mice. Evaluation of LVEF, %FS and the left ventricular wall thicknesses revealed no significant difference between *Clcn3*$^{-/-}$ mice and their heterozygous or wild type littermates. These results indicate that ClC-3 deletion does not affect the basic electrophysiological and hemodynamic performance of the mouse. Therefore, ClC-3 does not appear to contribute significantly to cardiovascular function at rest. This is consistent with the very limited basal VRCC activity under physiological conditions. VRCCs or ClC-3 channels may be activated, however, under stressed conditions [21-23, 42]. Cardiovascular stress in response to treadmill exercise is frequently used to detect cardiac abnormalities that are not readily apparent at rest. Therefore, we combined the telemetric technique with a treadmill exercise protocol to quantify the electrophysiological performance of *Clcn3*$^{-/-}$ mice under stress in a nonrestrained manner [43]. While exercise increased HR and decreased QRS and QT intervals to identical levels in both *Clcn3*$^{+/+}$ and *Clcn3*$^{+/-}$ mice the same exercise training increased HR to lesser extent and failed to change QRS and QT intervals in *Clcn3*$^{-/-}$ mice. These results suggest that ClC-3 channels play a much more prominent role in the regulation of cardiac electric activity under stressed conditions than at rest. Although activation of VRCCs will contribute both inward (Cl^- efflux) and outward (Cl^- influx) currents during the normal cardiac cycle it will have more significant effects at positive potentials to cause a repolarization and shortening of the action potential duration (APD) compared with smaller depolarizing effects at negative potentials near the resting membrane potential due to the stronger outwardly rectifying property of the ClC-3 currents [22, 42, 44]. A faster repolarization phase and shorter APD caused by activation of ClC-3 channels may explain why QRS and QT intervals were shortened in *Clcn3*$^{+/-}$ and *Clcn3*$^{+/+}$ mice but not in *Clcn3*$^{-/-}$ mice under stressed conditions. The failure of exercise to increase HR in *Clcn3*$^{-/-}$ mice to the same level as that in *Clcn3*$^{+/-}$ and *Clcn3*$^{+/+}$ mice may be, at least in part, due to the decrease in the inward depolarizing current and also the outward repolarizing current. Since $I_{Cl,swell}$ was also found in sino-atrial (SA) nodal cells, ClC-3 channels may play a significant role in the pacemaker function in these cells [42]. Disruption of ClC-3 in the SA nodal cells may therefore also lead to the failure to respond to positive chronotropic effect of exercise in *Clcn3*$^{-/-}$ mice. These data provide the first *in vivo* experimental evidence for the functional role of VRCCs in cardiac electrophysiology and hemodynamics.

Functional role of VRCCs in eIPC and swIPC

Using the *in vivo* models of eIPC and swIPC on genetically engineered mice and combined echocardiography and histological analyses we found in this study that ClC-3 encoded VRCCs may play an important cardioprotective role in swIPC but they may not contribute significantly to the eIPC protection. These findings are consistent in general with previous studies in terms of that VRCCs play a cardioprotective role in IPC.

Diaz et al. observed that several Cl^- channel blockers abolished IPC protection caused by hypoosmotic stress, ischemia/reperfusion, and pharmacological agents in isolated rabbit heart, implicating a functional role of VRCCs in eIPC [11-13]. Using the same IPC model and Cl^- channel blockers Heusch et al. failed to replicate the same results, raising the doubt about the causal role of Cl^- channels in IPC [15, 16]. In the mouse *in vivo* IPC model, we found that targeted disruption of ClC-3, which significantly altered endogenous VRCCs in mouse heart [35], did not affect the cardioprotective effect of eIPC. Our results, therefore, are in agreement with Heusch et al. and do not support a causal role of VRCCs in eIPC either. However, it is clear that the swIPC-induced cardioprotection was abolished by ClC-3 disruption, and thus our results strongly support the notion of that VRCCs are important mediators in IPC. Some of the discrepancies between our results and those of Diaz et al. and Heusch et al. may be due to the differences in species (mouse vs rabbit) and IPC models (*in vivo* vs *in vitro*) [11-13, 15, 16].

Functional role of VRCCs in cell volume regulation and cell death

Recent studies have shown that IPC protects myocardium against infarction through inhibition of apoptosis and limitation of necrosis [6, 7, 40, 45]. But it remains unclear how much the contribution of each of the two forms of cell death to ischemia/reperfusion-induced myocardial damage and infarction and whether the beneficial effects of eIPC and swIPC are mediated by similar or different signal transduction pathways involved in necrosis or apoptosis. Necrotic cell death, i.e., cell rupture is paralleled by irreversible isosmotic cell swelling or NVI, which is caused by ATP depletion under conditions of injury, hypoxia, ischaemia, or acidosis. Isosmotic cell shrinkage or apoptotic cell volume decrease (AVD) is an integral part of apoptosis. Both NVI and AVD have been found to be closely regulated by VRCCs. In the face of anisotonic perturbations, the ability of the cell to effectively control its internal environment and cell volume by mechanisms of RVD or RVI after osmotic swelling or shrinkage, respectively, is critical for cell survival under pathophysiological conditions. Dysfunction of RVD or RVI due to impairment of VRCC function causes persistent cell swelling or shrinkage and ultimately cell death through NVI or AVD, respectively. When the cell volume regulatory mechanism is altered, stress such as ischemia/reperfusion would lead to enhanced myocardial infarction. A close link between apoptosis and the activity of native $I_{Cl,swell}$ and the expression of ClC-3 protein has been established previously in both cardiac and non-cardiac cells and tissues [8-10, 25, 46]. In a recent study, for example, Lemonnier and colleagues [9, 25] found that overexpression of Bcl-2 oncoprotein, a key antiapoptotic regulator, in lymph node carcinoma of the prostate (LNCaP) prostate cancer epithelial cells resulted in the doubling of VRCC-carried $I_{Cl,swell}$ and weakened $I_{Cl,swell}$ inhibition by store-operated Ca^{2+} channel (SOC)-transported Ca^{2+}. This was accompanied by substantial up-regulation of ClC-3 protein. Furthermore, treatment of wild-type LNCaP cells with epidermal growth factor, which promotes cell proliferation, resulted in the enhancement of endogenous Bcl-2 expression and associated increases in ClC-3 levels and $I_{Cl,swell}$ magnitude. ClC-3-specific antibody suppressed $I_{Cl,swell}$ in the wild-type and Bcl-2-overexpressing LNCaP cells. Therefore, Bcl-2-induced up-regulation of $I_{Cl,swell}$, caused by enhanced expression of ClC-3 and weaker negative control from SOC-transported Ca^{2+}, may strengthen the ability of the cells to handle cell volume perturbations and thereby promote their survival and diminish their proapoptotic potential. On the other hand, in an *in vivo* rat heart global I/R model, Mizoguchi et al. found that intravenous administration of Cl^- channel blockers DIDS and NPPB were as potent as a broad-spectrum caspase inhibitor, benzoyloxycarbonyl-Asp-CH2OC(O)-2,6-dichlorobenzene (Z-Asp-DCB), in reducing myocardial DNA fragmentation, caspase activation, and improving cardiac contractile function after acute ischemia and 24-hr *in vivo* reperfusion [46]. These results suggest that inhibition of VRCCs is also effective for preventing apoptosis and elevation of caspase-3 activity during acute cardiac I/R injury. In eIPC, activation of PKC may inhibit the activation of VRCCs and thus prevent cell death. This may explain why ClC-3 deletion actually did not prevent the cardioprotective effect of eIPC. In swIPC, cell swelling-induced increase in VRCCs' function and upregulation of ClC-3 expression would strengthen the RVD mechanism and prevent the NVI process of cardiac cells. Activation of VRCCs would increase the apoptotic resistant of the cell in the face of further ischemic perturbations. If brief periods of ischemia and reperfusion cause the upregulation of ClC-3 expression the effects of its anti-apoptotic properties would require time to manifest. This may explain why the late phase of IPC is affected but not the early phase of IPC in ClC-3 knockout mice. The differential effects of ClC-3 disruption on eIPC and swIPC may reflect the involvement of VRCCs in different mechanisms for the cardioprotection in eIPC and

swIPC. Thus, VRCCs may play a cell-rescuing role in the necrotic process by ensuring RVD after cell swelling induced by necrotic insults, whereas isotonic activation of VRCCs may play a cell-killing role in the apoptotic process by triggering AVD following stimulation with apoptosis inducers.

Acknowledgements

This study was supported by grants from National Institutes of Health (NIH), National Center for Research Resources (NCRR) P20RR15581, National Heart, Lung, and Blood Institute Grant HL63914 and HL106256 (to D.D.D.) and HL62483 (to F.S.L.), and American Heart Association Western States Affiliate Grant-in-Aid #11GRNT7610161 (to D.D.D.) Tammy Y. Yao was supported by an Undergraduate Research Award from American Heart Association Western States Affiliate. The authors wish to thank Dr. William Hatton, Dr. Hongling Tian, Paul Scowen and Rebecca Evans for technical assistance.

References

1 Murry CE, Jennings RB, Reimer KA: Preconditioning with ischemia: a delay of lethal cell injury in ischemic myocardium. Circulation 1986;74:1124-1136.

2 Guo Y, Wu WJ, Qiu Y, Tang XL, Yang Z, Bolli R: Demonstration of an early and a late phase of ischemic preconditioning in mice. Am J Physiol 1998;275:H1375-H1387.

3 Bolli R: Cardioprotective function of inducible nitric oxide synthase and role of nitric oxide in myocardial ischemia and preconditioning: an overview of a decade of research. J Mol Cell Cardiol 2001;33:1897-1918.

4 Downey JM, Cohen MV: Reducing infarct size in the setting of acute myocardial infarction. Prog Cardiovasc Dis 2006;48:363-371.

5 Hausenloy DJ, Yellon DM: The therapeutic potential of ischemic conditioning: an update. Nat Rev Cardiol 2011;8:619-629.

6 Zhao ZQ, Vinten-Johansen J: Myocardial apoptosis and ischemic preconditioning. Cardiovasc Res 2002;55:438-455.

7 Lopez-Neblina F, Toledo AH, Toledo-Pereyra LH: Molecular biology of apoptosis in ischemia and reperfusion. J Invest Surg 2005;18:335-350.

8 Guan YY, Wang GL, Zhou JG: The ClC-3 Cl- channel in cell volume regulation, proliferation and apoptosis in vascular smooth muscle cells. Trends Pharmacol Sci 2006;27:290-296.

9 Lemonnier L, Lazarenko R, Shuba Y, Thebault S, Roudbaraki M, Lepage G, Prevarskaya N, Skryma R: Alterations in the regulatory volume decrease (RVD) and swelling-activated Cl^- current associated with neuroendocrine differentiation of prostate cancer epithelial cells. Endocr Relat Cancer 2005;12:335-349.

10 Okada Y, Shimizu T, Maeno E, Tanabe S, Wang X, Takahashi N: Volume-sensitive chloride channels involved in apoptotic volume decrease and cell death. J Membr Biol 2006;209:21-29.

11 Diaz RJ, Losito VA, Mao GD, Ford MK, Backx PH, Wilson GJ: Chloride channel inhibition blocks the protection of ischemic preconditioning and hypo-osmotic stress in rabbit ventricular myocardium. Circ Res 1999;84:763-775.

12 Batthish M, Diaz RJ, Zeng HP, Backx PH, Wilson GJ: Pharmacological preconditioning in rabbit myocardium is blocked by chloride channel inhibition. Cardiovasc Res 2002;55:660-671.

13 Diaz RJ, Batthish M, Backx PH, Wilson GJ: Chloride channel inhibition does block the protection of ischemic preconditioning in myocardium. J Mol Cell Cardiol 2001;33:1887-1889.

14 Diaz RJ, Armstrong SC, Batthish M, Backx PH, Ganote CE, Wilson GJ: Enhanced cell volume regulation: a key protective mechanism of ischemic preconditioning in rabbit ventricular myocytes. J Mol Cell Cardiol 2003;35:45-58.

15 Heusch G, Cohen MV, Downey JM: Ischemic preconditioning through opening of swelling-activated chloride channels? Circ Res 12-7-2001;89:E48.

16 Heusch G, Liu GS, Rose J, Cohen MV, Downey JM: No confirmation for a causal role of volume-regulated chloride channels in ischemic preconditioning in rabbits. J Mol Cell Cardiol 2000;32:2279-2285.
17 Comes N, Gasull X, Gual A, Borras T: Differential expression of the human chloride channel genes in the trabecular meshwork under stress conditions. Exp Eye Res 2005;80:801-813.
18 Duan D, Winter C, Cowley S, Hume JR, Horowitz B: Molecular identification of a volume-regulated chloride channel. Nature 1997;390:417-421.
19 Duan D, Cowley S, Horowitz B, Hume JR: A serine residue in ClC-3 links phosphorylation-dephosphorylation to chloride channel regulation by cell volume. J Gen Physiol 1999;113:57-70.
20 Duan D, Zhong J, Hermoso M, Satterwhite CM, Rossow CF, Hatton WJ, Yamboliev I, Horowitz B, Hume JR: Functional inhibition of native volume-sensitive outwardly rectifying anion channels in muscle cells and Xenopus oocytes by anti-ClC-3 antibody. J Physiol 2001;531:437-444.
21 Duan D: Phenomics of cardiac chloride channels: the systematic study of chloride channel function in the heart. J Physiol 2009;587:2163-2177.
22 Duan DD: The ClC-3 chloride channels in cardiovascular disease. Acta Pharmacol Sin 2011;32:675-684.
23 Duan DY, Liu LL, Bozeat N, Huang ZM, Xiang SY, Wang GL, Ye L, Hume JR: Functional role of anion channels in cardiac diseases. Acta Pharmacol Sin 2005;26:265-278.
24 Jin NG, Kim JK, Yang DK, Cho SJ, Kim JM, Koh EJ, Jung HC, So I, Kim KW: Fundamental role of ClC-3 in volume-sensitive Cl^- channel function and cell volume regulation in AGS cells. Am J Physiol Gastrointest Liver Physiol 2003;285:G938-G948.
25 Lemonnier L, Shuba Y, Crepin A, Roudbaraki M, Slomianny C, Mauroy B, Nilius B, Prevarskaya N, Skryma R: Bcl-2-dependent modulation of swelling-activated Cl^- current and ClC-3 expression in human prostate cancer epithelial cells. Cancer Res 2004;64:4841-4848.
26 Moreland JG, Davis AP, Bailey G, Nauseef WM, Lamb FS: Anion channels, including ClC-3, are required for normal neutrophil oxidative function, phagocytosis, and transendothelial migration. J Biol Chem 2006;281:12277-12288.
27 Sontheimer H: An unexpected role for ion channels in brain tumor metastasis. Exp Biol Med (Maywood) 2008;233:779-791.
28 Xiong D, Wang GX, Burkin DJ, Yamboliev IA, Singer CA, Rawat S, Scowen P, Evans R, Ye L, Hatton WJ, Tian H, Keller PS, McCloskey DT, Duan D, Hume JR: Cardiac-specific overexpression of the human short ClC-3 chloride channel isoform in mice. Clin Exp Pharmacol Physiol 2009;36:386-93.
29 Zhang HN, Zhou JG, Qiu QY, Ren JL, Guan YY: ClC-3 chloride channel prevents apoptosis induced by thapsigargin in PC12 cells. Apoptosis 2006;11:327-336.
30 Zhou JG, Ren JL, Qiu QY, He H, Guan YY: Regulation of intracellular Cl- concentration through volume-regulated ClC-3 chloride channels in A10 vascular smooth muscle cells. J Biol Chem 2005;280:7301-7308.
31 Chen H, Liu LL, Ye LL, McGuckin C, Tamowski S, Scowen P, Tian H, Murray K, Hatton WJ, Duan D: Targeted inactivation of cystic fibrosis transmembrane conductance regulator chloride channel gene prevents ischemic preconditioning in isolated mouse heart. Circulation 2004;110:700-704.
32 Dickerson LW, Bonthius DJ, Schutte BC, Yang B, Barna TJ, Bailey MC, Nehrke K, Williamson RA, Lamb FS: Altered GABAergic function accompanies hippocampal degeneration in mice lacking ClC-3 voltage-gated chloride channels. Brain Res 2002;958:227-250.
33 Xiang SY, Ye LL, Duan LL, Liu LH, Ge ZD, Auchampach JA, Gross GJ, Duan DD: Characterization of a critical role for CFTR chloride channels in cardioprotection against ischemia/reperfusion injury. Acta Pharmacol Sin 2011;32:824-833.
34 Duan D, Ye L, Britton F, Horowitz B, Hume JR: UltraRapid communications : A novel anionic inward rectifier in native cardiac myocytes. Circ Res 2000;86:485.
35 Yamamoto-Mizuma S, Wang GX, Liu LL, Schegg K, Hatton WJ, Duan D, Horowitz TL, Lamb FS, Hume JR: Altered properties of volume-sensitive osmolyte and anion channels (VSOACs) and membrane protein expression in cardiac and smooth muscle myocytes from $Clcn3^{-/-}$ mice. J Physiol 2004;557:439-456.
36 Isenberg G, Klockner U: Calcium tolerant ventricular myocytes prepared by preincubation in a „KB medium". Pflugers Arch 1982;395:6-18.
37 Duan D, Fermini B, Nattel S: Alpha-adrenergic control of volume-regulated Cl- currents in rabbit atrial myocytes. Characterization of a novel ionic regulatory mechanism. Circ Res 1995;77:379-393.
38 Mitchell GF, Jeron A, Koren G: Measurement of heart rate and Q-T interval in the conscious mouse. Am J Physiol 1998;274:H747-H751.
39 Sahn DJ, DeMaria A, Kisslo J, Weyman A: Recommendations regarding quantitation in M-mode echocardiography: results of a survey of echocardiographic measurements. Circulation 1978;58:1072-1083.
40 Vohra HA, Galinanes M: Myocardial preconditioning against ischemia-induced apoptosis and necrosis in man. J Surg Res 2006;134:138-144.
41 Stobrawa SM, Breiderhoff T, Takamori S, Engel D, Schweizer M, Zdebik AA, Bosl MR, Ruether K, Jahn H, Draguhn A, Jahn R, Jentsch TJ: Disruption of ClC-3, a chloride channel expressed on synaptic vesicles, leads to a loss of the hippocampus. Neuron 2001;29:185-196.
42 Baumgarten CM, Clemo HF: Swelling-activated chloride channels in cardiac physiology and pathophysiology. Prog Biophys Mol Biol 2003;82:25-42.
43 Fewell JG, Osinska H, Klevitsky R, Ng W, Sfyris G, Bahrehmand F, Robbins J: A treadmill exercise regimen for identifying cardiovascular phenotypes in transgenic mice. Am J Physiol 1997;273:H1595-H1605.
44 Hume JR, Duan D, Collier ML, Yamazaki J, Horowitz B: Anion transport in heart. Physiol Rev 2000;80:31-81.
45 Vohra HA, Fowler AG, Galinanes M: Preconditioning with cardioplegia is more effective in reducing apoptosis than is preconditioning with ischemia in the human myocardium. Ann N Y Acad Sci 2003;1010:721-727.
46 Mizoguchi K, Maeta H, Yamamoto A, Oe M, Kosaka H: Amelioration of myocardial global ischemia/reperfusion injury with volume-regulatory chloride channel inhibitors in vivo. Transplantation 2002;73:1185-1193.